

## Nuclear Clusters in Astrophysics - *Experimental Approach to Cluster Structure* -

---

**Shigeru KUBONO<sup>1</sup>**

*Center for Nuclear Study (CNS), University of Tokyo, Wako Branch at RIKEN  
2-1 Hirosawa, Wako, Saitama, 351-0198 Japan  
E-mail: kubono@cns.s.u-tokyo.ac.jp*

The role of nuclear clustering is discussed for nucleosynthesis in stellar evolution with the previously proposed Cluster Nucleosynthesis Diagram (CND). I mainly discuss  $\alpha$ -cluster nature for nucleosynthesis, which can be investigated by two experimental methods, alpha resonant elastic scattering and direct alpha transfer reactions. Specifically, we present the important role of  $\alpha$  cluster resonance in the  $(\alpha,p)$  reactions. The applicability of direct cluster transfer reactions are also discussed in terms of the reaction mechanism. Some possibilities are also discussed for the investigation of O- and C-burning with massive transfer reactions.

*VI European Summer School on Experimental Nuclear Astrophysics  
Acireale Italy  
September 18-27, 2011*

---

<sup>1</sup> Speaker

### 1. Nuclear Clusters in Nucleosynthesis

Nuclear reactions play a key role for the evolution of stars of producing large energies as well as new elements. After hydrostatic hydrogen burning, the helium ashes become the fuel in the next stage, called helium burning. Subsequent burning processes involve C, O and Si as fuels until the iron core formation [1].

Figure 1 depicts the idea of these nuclear burning processes in stars till the epoch of the iron-core formation. This diagram was proposed before [2,3] to give a natural way of understanding stellar nucleosynthesis. This diagram explains the dynamics of nucleosynthesis in nature. This is very much like the Ikeda diagram for cluster physics, which suggests presence of cluster states near the cluster threshold. This is called the cluster threshold rule. The important fact here is that this is just the energy region of nucleosynthesis that takes place in the universe, because the relevant thermal energies of stellar reactions are small. Therefore, one should expect that states with a large parentage of cluster configuration contribute significantly to the nucleosynthesis.

The first step of the helium burning is the synthesis of  $^{12}\text{C}$  by capture of an  $\alpha$  particle on  $^8\text{Be}$  through  $\alpha$ -cluster states in  $^{12}\text{C}$ . The second step is the  $^{12}\text{C}(\alpha,\gamma)^{16}\text{O}$  reaction. After the helium burning, the ashes of helium burning,  $^{12}\text{C}$  and  $^{16}\text{O}$ , become the fuel and lead to C- and O-burning, which largely go through the fusion reactions emitting  $\alpha$  particles, together with subsequent  $\alpha$ -induced reactions on even-even sd-shell nuclei. Eventually, silicon burning begins from  $^{28}\text{Si}$  seed material with successive  $(\alpha,\gamma)$  and  $(\alpha,p)$  reactions together with photo-disintegration of  $^{28}\text{Si}$ , etc. Here, an interesting observation is that in nuclear physics, one may add excitation energy to the nuclear system to see the evolution of clusters. For instance, in  $^{24}\text{Mg}$  there appears an  $\alpha$ -cluster state, then a  $2\alpha$ -cluster state or  $^{12}\text{C}+^{12}\text{C}$  molecular state, etc.,

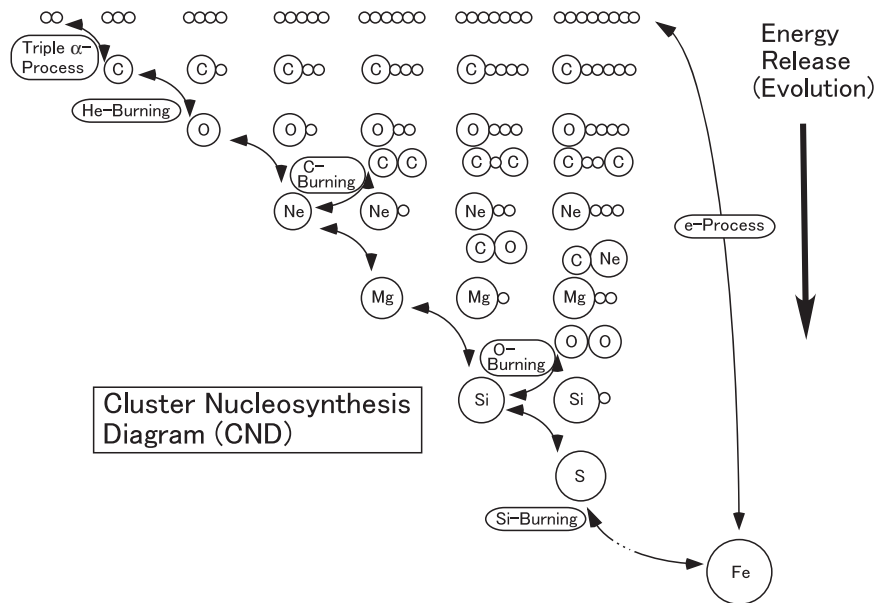


**FIGURE 1.** Cluster Nucleosynthesis Diagram (CND) for nucleosynthesis along the stellar evolution [2,3].

whereas nucleosynthesis in nature goes in other way around. Nucleosynthesis here is a series of successive processes of crushing clusters to form a one-body system, gaining the difference in binding energies as thermal energy. Thus, the vertical axis in the figure should be regarded as the energy release during the progression of stellar evolution.

Here, the most important fact is that the CND diagram arises naturally from "the cluster threshold rule" that has been long recognized and has been an important guide-line for finding cluster states in nuclei, as discussed above.

The cluster properties will be studied experimentally by two methods, resonant  $\alpha$  elastic scattering study using the thick target method, and a direct  $\alpha$  transfer reactions such as ( ${}^6\text{Li},d$ ) and ( ${}^7\text{Li},t$ ) reactions. Recently, we have been working on a series of ( $\alpha,p$ ) stellar reactions such as  ${}^{21}\text{Na}(\alpha,p)$  with the thick target method, and identified that the strong resonant feature observed in the ( $\alpha,p$ ) cross sections are due to the  $\alpha$  resonances just above the  $\alpha$  threshold. This fact clearly indicates that the  $\alpha$  resonance has a decisive role in the ( $\alpha,p$ ) stellar reaction as expected.

We discuss specifically experimental studies of a cluster structure in nuclei relevant to nucleosynthesis in the universe. In section 2, low energy resonant scattering of alpha particles are discussed, direct alpha transfer reactions and the reaction mechanism in section 3, possible resonance studies with heavier  $4n$  nuclei in section 4, and the summary in section 5.

## 2. $\alpha$ Resonant Elastic Scattering

Since  ${}^4\text{He}$  is the second most abundant isotope, there are many astronomical environments where  $\alpha$  induced reactions play an important role in the universe. They include ( $\alpha,\gamma$ ), ( $\alpha,p$ ) and ( $\alpha,n$ ) reactions. Because of the charge of  $\alpha$  particle,  $\alpha$ -induced stellar reactions usually play an important role at higher energies than proton induced reactions, although in the low mass region, there are some specific alpha induced reactions even at low energies. But these reactions mostly have small alpha reduced widths, which imply that these states are important but not the "cluster states" considered in detail here.

### 2.1 Thick Target Method for Scattering of Unstable Nuclei

Since we study explosive nucleosynthesis with alpha particles, major reactions involve short-lived unstable nuclei. Therefore, we use the inverse kinematics, i.e., beams of unstable heavy nuclei on a thick target of  ${}^4\text{He}$  [4] to study  $\alpha$  resonances.

Low-energy RI beams can be obtained by two methods; one is an ISOL based reacceleration system, and the other one is an in-flight RI beam separator with primary heavy ion beams. Figure 1 shows an example of the latter type, called CRIB, installed by the Center for Nuclear Study, University of Tokyo (CNS) in the RIKEN RIBF facility [5,6]. Since available production target thickness is small, RI beam intensities are limited. However, it has been greatly improved by a total system development for CRIB. By recirculating cooled gas

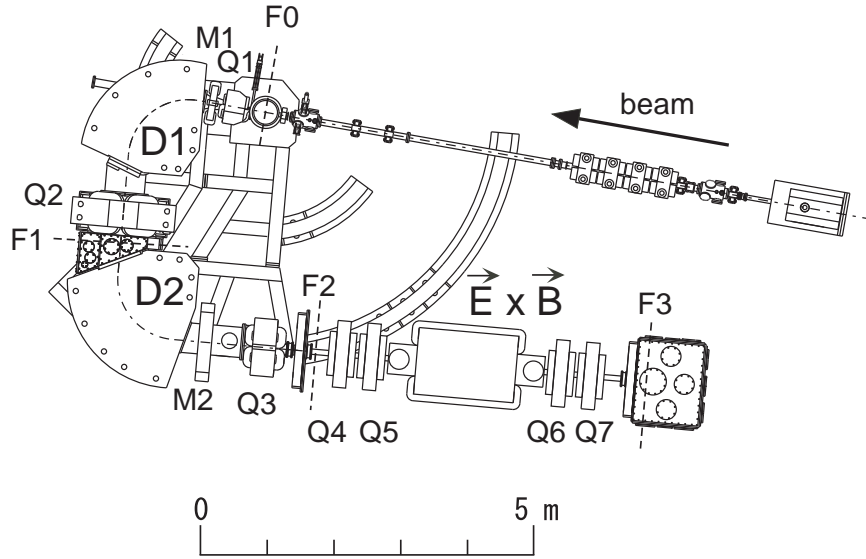


**FIGURE 2.** The plane view of the low-energy RI beam separator, CRIB. High-intensity primary heavy ion beams are provided by the AVF cyclotron of RIKEN.

for the production target [7], high-intensity RI beams are now available, such as  $3 \times 10^8$  pps of  ${}^7\text{Be}$  of high purity which is provided by a Wien-filter installed at end.

I will discuss next two recent experimental results obtained at the CRIB facility.

### 2.2 ${}^7\text{Li}+\alpha$ Elastic Scattering

Recently,  ${}^7\text{Li}+\alpha$  elastic scattering was studied in inverse kinematics with a thick He gas target in order to investigate  $\alpha$ -cluster structure in  $A=11$  nuclei [8] and the nucleosynthesis of  ${}^7\text{Li}(\alpha,\gamma){}^{11}\text{B}$ , which

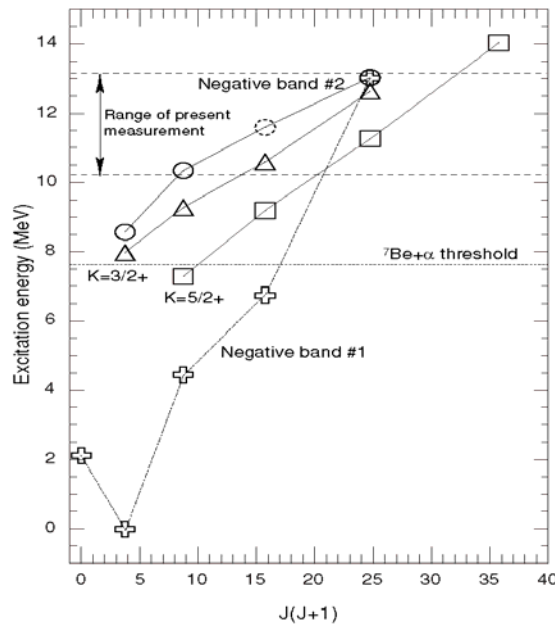


**FIGURE 3.** New resonances are plotted for a possible negative parity band #2 [8].

is considered to be relevant to  $^{11}\text{B}$  production in the neutrino process in type II supernovae [9].

The experiment was performed at the CRIB facility with a  $^7\text{Li}$  beam and an extended He target. The excitation function of the  $^7\text{Li}+\alpha$  elastic scattering cross sections was measured at 180 degrees [8]. New resonances of negative parity observed at 10.34 MeV ( $5/2^-$ ) and 13.03 MeV ( $9/2^-$ ) suggest a new rotational band, which is consistent with a rotational band of a dilute cluster state predicted by an anti-symmetrized molecular dynamics (AMD) method [10].

### 2.3 $^{21}\text{Na}(\alpha, p)^{24}\text{Mg}$ Stellar Reaction

At higher temperature and higher density condition of hydrogen and helium rich material,  $(\alpha, p)$  reactions dominate the burning process, which is called the  $\alpha p$ -process. This process would play a crucial role in various stage of the stellar evolution. For instance, the  $^{14}\text{O}(\alpha, p)^{17}\text{F}$  [11,12] and  $^{18}\text{Ne}(\alpha, p)^{21}\text{Na}$  reactions are crucial for ignition of X-ray bursts, which still await more experimental investigation. The  $\alpha p$ -process is also considered to play a crucial role in the low mass regions in the vp-process which will take place at the very early epoch of type II supernovae [13-15]. After production of CNO elements in the vp-process, the next step of the nucleosynthesis is a flow out from the CNO region to the heavier element region. The  $^{21}\text{Na}(\alpha, p)$  stellar reaction might plays a crucial role for synthesis of the long-lived nuclei  $^{44}\text{Ti}$  and  $^{22}\text{Na}$  [16,17], the target nuclei of nuclear gamma ray observations [18]. There was only a data of  $^{21}\text{Na}(\alpha, p_0)^{24}\text{Mg}(\text{g.s.})$  which was measured by the activation method with the time reverse reaction [19].

A beautiful experimental result was obtained recently for the  $^{21}\text{Na}(\alpha, p)$  stellar reaction [20]. A  $^{21}\text{Na}$  beam was obtained from the CRIB separator. As can be seen in Fig. 4, the four prominent peaks appear to correspond to the peaks in the excitation function of the  $^{21}\text{Na}(\alpha, p_0)^{24}\text{Mg}$  reaction, which was measured by the time reverse reaction using an activation method [19], although the correspondences are not perfect in detail.

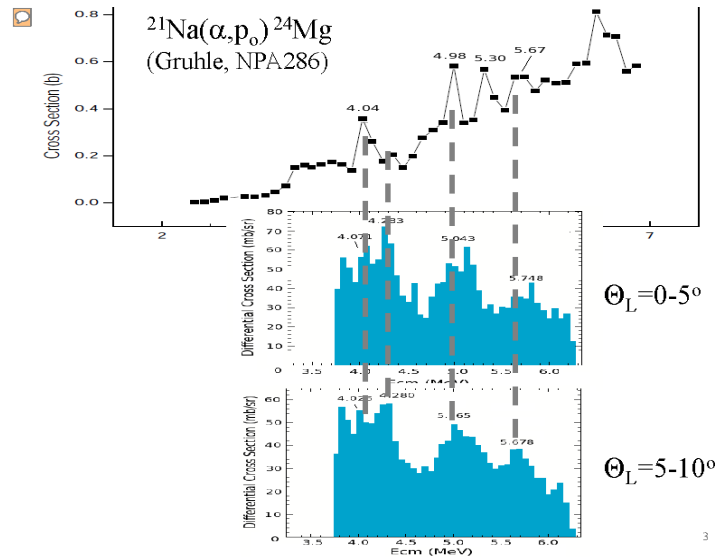


**FIGURE 4.**  $\alpha$  resonant elastic scattering [20] and the  $^{21}\text{Na}(\alpha, p_0)^{24}\text{Mg}$  reaction cross sections [19].

The R-matrix analysis has revealed that all these resonances have quite large  $\alpha$  reduced widths which exhausted large fractions of the Wigner limits. This result implies that  $\alpha$ -resonances have a major role for the  $^{21}\text{Na}(\alpha, p)$  reaction rate, as expected by the CND [2,3]. We also have succeeded to measure directly the cross sections of  $^{21}\text{Na}(\alpha, p)^{24}\text{Mg}$ , which show much larger cross sections than those accepted before [20].

### 3. Direct $\alpha$ Transfer Reactions

The resonant elastic scattering method discussed above is limited in sensitivity at low scattering energies because the Coulomb interaction dominates the cross sections for charged particle scattering. Since the elastic scattering amplitude is a coherent sum of the Coulomb scattering term and the resonant term, it is difficult to observe resonance peaks near the particle threshold. On the other hand, direct transfer reactions can excite both bound and resonant states with a cross sections proportional to the spectroscopic factor, virtually free from the Coulomb interaction.

Let me compare the two methods in a little more detail. The alpha width  $\Gamma_\alpha$  which can be obtained by the elastic resonant scattering, as was discussed in the previous section, is related to the reduced width  $\gamma_\alpha^2$  as follows;

$$\Gamma_\alpha = 2 \frac{k_\alpha R}{|F_\ell(k_\alpha R)|^2 + |G_\ell(k_\alpha R)|^2} \gamma_\alpha^2 ,$$

where  $F_\ell$  and  $G_\ell$  are the regular and irregular Coulomb wave functions, respectively, and  $R$  is the channel radius. One can derive the  $\alpha$  spectroscopic factor  $S_\alpha$  from the DWBA analysis of the angular distribution of the direct  $\alpha$  transfer reaction [21],

$$S_\alpha = \left( \frac{d\sigma}{d\Omega} \right)_{\text{EXP}} / \left( \frac{d\sigma}{d\Omega} \right)_{\text{DWBA}} ,$$

where  $(d\sigma/d\Omega)_{\text{EXP}}$ ,  $(d\sigma/d\Omega)_{\text{DWBA}}$  are the experimental and theoretical differential cross sections. This spectroscopic factor is directly related to the reduced width defined above by;

$$\gamma_\alpha^2 = \frac{3\hbar^2}{2\mu R^2} S_\alpha ,$$

where  $\mu$  is the reduced mass.

Specifically, the direct transfer reactions are useful for investigating states near and just below the threshold, where observed  $\Gamma_\alpha$ 's are so small, but the  $\gamma_\alpha^2$  are not so small. Generally speaking, however, DWBA should not be used for a transition that has so small  $S_\alpha$  because it might have more contributions from non-direct processes. In this section, I will mainly discuss the reaction mechanism of the “direct transfer reactions”, and the applicability for spectroscopy.

#### 3.1 Multi-Step Processes

The reaction mechanism of “direct process” at around 10 MeV/u or below were extensively studied in 1970s and 1980s. Non-direct process contributions are not avoidable

even under the optimum conditions for any particle transfer reactions. For instance, even elastic scattering was found to have a strong coupling to the band members in deformed nuclei, which alters the Fresnel type angular distribution. A long standing problem of absolute cross sections of two-nucleon transfer reactions, like (p,t), and ( $^{18}\text{O}$ ,  $^{16}\text{O}$ ) [22,23], have been identified by successive processes. Even for the cross sections of the ground state transitions of the ( $^{18}\text{O}$ ,  $^{16}\text{O}$ ) reactions the successive transfer contributions comprises nearly half of them.

Here, I demonstrate a typical one-nucleon transfer reaction at 52 MeV, where we have a good condition for a direct process, but have significant two-step contributions. Figure 5 displays the angular distributions of the  $^{40}\text{Ca}(p,d)^{39}\text{Ca}$  reaction for the 3.63 MeV  $9/2^-$  state and the 3.00 MeV  $3/2^-$  state in  $^{39}\text{Ca}$  [24]. We expect here a direct transfer process for the  $3/2^-$  state and multi-step processes for the  $9/2^-$  state. Because there is no  $h_{9/2}$  orbit near the ground state in  $^{40}\text{Ca}$ , the 3.63 MeV state is considered to be a weak coupled state of  $^{40}\text{Ca}(3^-) \times d_{3/2}^{-1}$ . However, we expect a direct neutron transfer for the  $3/2^-$  state because there are two-particle two-hole components in  $^{40}\text{Ca}(\text{g.s.})$ . Actually, the two-step DWBA calculation [25], which includes the second order Born terms, explains the shape of the strange angular distribution of the  $9/2^-$  state as well as the absolute cross sections. Here, the calculation was made including the two step processes of  $^{40}\text{Ca}(p,p')^{40}\text{Ca}(3^-)(p,d)^{39}\text{Ca}(9/2^-)$  and  $^{40}\text{Ca}(p,d)^{39}\text{Ca}(\text{g.s.})(d,d')^{39}\text{Ca}(9/2^-)$ . Here, the transitions from the  $3^-$  to the  $9/2^-$  was assumed to be a  $d_{3/2}$  neutron transfer with a weak coupling scheme, and the optical potential parameters were obtained by fitting the elastic scattering. As can be seen in Fig. 5, the angular distribution shapes and the absolute cross sections were well explained by the two-step DWBA calculation. The right hand panel in Fig. 5 shows the (p,d) transition to the 3.00 MeV  $3/2^-$  state. Usually, one may assume a direct transition for the allowed transition of reasonable cross sections like the case here. The one-step DWBA calculation for the  $3/2^-$  state shows a poor fit to the data, as can be seen in Fig. 5. The angular

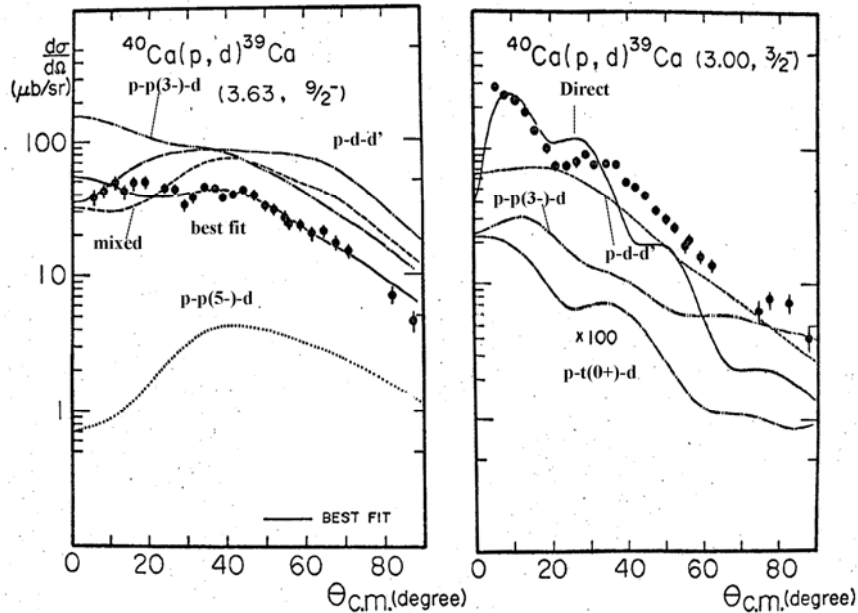


**FIGURE 5.** Angular distribution for the  $^{40}\text{Ca}(p,d)^{39}\text{Ca}(3.63\ 9/2^-)$  (left panel), and that for the  $^{40}\text{Ca}(p,d)^{39}\text{Ca}(3.00\ 3/2^-)$  (right panel), together with two-step DWBA calculations.

distributions can be better fitted by including the two-step processes,  $^{40}\text{Ca}(p,p')^{40}\text{Ca}(3^-)$  ( $p,d$ )  $^{39}\text{Ca}(3/2^-)$  and  $^{40}\text{Ca}(p,d)^{39}\text{Ca}(\text{g.s.})(d,d')^{39}\text{Ca}(3/2^-)$ . Here, the two-step contributions, as a weak-coupled state, were included together with the direct amplitude. The spectroscopic factor  $Sp_{3/2}$  obtained by the one-step DWBA analysis has to be reduced roughly by a factor of 4. Note that the cross section range of two-step processes is not so small in either the two transitions shown in Fig. 5. The present incident energy is reasonably high for direct reaction, but we still have to consider multi-step processes seriously to deduce correct spectroscopic information.

### 3.2 Direct and Non-Direct $\alpha$ Transfer Reactions

As discussed in the previous subsection, one has to pay full attention to the reaction mechanism when using direct reaction theory DWBA to extract the spectroscopic factor. This method, however, can sometimes be only the way to study  $\alpha$  structures for resonances which are located close to the alpha threshold or a sub-threshold resonance, because transfer reactions are almost free from the effect by the Coulomb penetrability near the threshold.

The direct  $\alpha$ -transfer reaction on  $^{13}\text{C}$  has received a lot of interest because of the  $^{13}\text{C}(\alpha,n)^{17}\text{O}$  stellar reaction which is believed to be the neutron source for the main s-process. The astrophysical problem is that the stellar reaction cross sections at helium burning temperature are not known. First, the  $^{13}\text{C}(^6\text{Li},d)^{17}\text{O}$  reaction was studied, at 60 MeV [26], and later the same reaction at much lower energies [27], and by other reactions  $^{13}\text{C}(^7\text{Li},t)^{17}\text{O}$  at 28 and 34 MeV [28].

These reactions were studied, except for the first one, at low energies. From the systematic studies in the 1970s and 1980, it is known that the reaction mechanism changes drastically in the energy region of 1 – 10 MeV/u. One needs to be very careful for the reaction mechanism

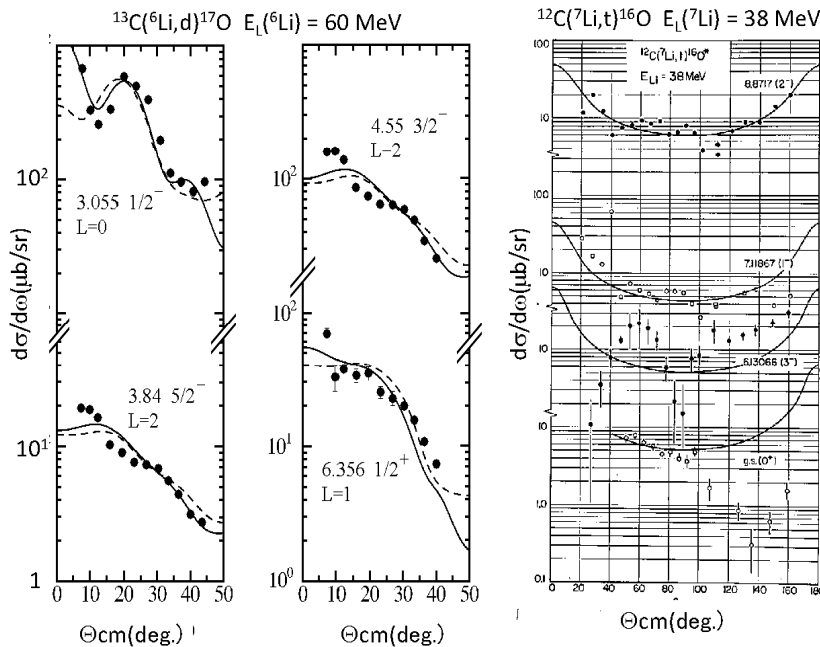


**FIGURE 6.** (a) Angular distributions for the  $^{13}\text{C}(^6\text{Li},d)$  reaction at 60 MeV [26], and (b) the  $^{12}\text{C}(^7\text{Li},t)^{16}\text{O}$  at 38 MeV [29].



associated. The fusion cross sections have a general trend that the cross sections change as a function of  $E_{\text{cm}}^{-1}$  [30], whereas the cross sections for quasi-elastic channels increase as the incident energy increases. Thus, the  $\alpha$ -transfer reactions at lower energies have a good chance to have significant amplitudes of non-direct processes in the transitions even for allowed transitions. For example, the unnatural-parity  $2^-$  state at 8.87 MeV was excited as large as other natural parity states in the  $^{12}\text{C}(^7\text{Li,t})^{16}\text{O}$  reaction at 38 MeV, as shown in the right hand panel in Fig. 6, and the angular distribution was nearly 90 degree symmetric [29]. Note that the direct  $\alpha$ -transfer reaction is completely forbidden for unnatural parity states. This clearly indicates that most  $(^7\text{Li,t})$  reactions even for natural-parity states at this energy have a considerable compound process contribution. This problem also applies when using the ANC method, and the same consideration needs to be made carefully.

#### 4. Molecular States of $^{16}\text{O} + ^{16}\text{O}$ for O-Burning

Recently, the C- burning and O-burning processes have re-attracted nuclear astrophysicists very much. New measurements of the fusion cross sections of  $^{12}\text{C} + ^{12}\text{C}$  at lower energies than that known before indicates cross sections which is quite different from the high-energy extrapolation toward the Gamow window at low energy. For studies of these burning processes, it is important to study molecular states as suggested by the CND diagram. Due to the cluster threshold rule, we might have a large chance that the molecular resonances are located near the  $^{16}\text{O} + ^{16}\text{O}$  threshold and influence the fusion cross sections seriously. I just note that, interestingly, such a study was performed for finding possible molecular state of  $^{16}\text{O} + ^{16}\text{O}$  some time ago [31].

The  $^{16}\text{O}(^{20}\text{Ne},\alpha_1)^{32}\text{S}^*(\alpha_2)^{28}\text{Si}$  reaction was chosen to study possible molecular state of  $^{16}\text{O} + ^{16}\text{O}$  in  $^{32}\text{S}$  near the  $^{16}\text{O} + ^{16}\text{O}$  threshold, because the ground state of  $^{20}\text{Ne}$  has a reasonably large parentage of  $\alpha + ^{16}\text{O}$  configuration. The angular correlation functions of  $\alpha_1$  and  $\alpha_2$  provided successfully a unique spin assignment for the resonances seen in the  $\alpha_1$  spectrum. The result indicates presence of possible molecular resonances around the  $^{16}\text{O} + ^{16}\text{O}$  threshold. Clearly, such resonances would affect to the reaction rate of O burning. It is suggested that indirect methods such as the Trojan Horse method [32] would be interesting for further investigation.

#### 5. Summary

We discussed the role of nuclear clusters for astrophysics, especially of alpha clusters for nucleosynthesis at high temperatures with our new  $(\alpha,p)$  experiments using low-energy RI beams from the CRIB facility. We have measured successfully the  $(\alpha,p)$  cross sections directly at the temperatures of interest, and the  $(\alpha,p)$  cross sections have been shown to be characterized strongly by alpha cluster resonances, as expected by the Cluster Nucleosynthesis Diagram.

The reaction mechanism of “direct transfer reaction” was also discussed to deduce proper spectroscopic factors partly by using two-step DWBA calculations. It is demonstrated that a special care should be paid for non-direct processes when one deduces spectroscopic information from “the direct reactions”.

A possibility of studying molecular resonances was also discussed for C- and O-burning.

## References

- [1] Proc. *Origin of Matter and Evolution of Galaxies 2010*, eds. I. Tanihata, T. Shima, H.J. Ong, A. Tamii, T. Kishimoto, H. Toki, T. Kajino, and S. Kubono, *AIP Conf. Proc.* **1269** (2010).  
Proc. *Origin of Matter and Evolution of Galaxies 2007*, eds. by T. Suda, T. Nozawa, A. Ohnishi, K. Kato, M. Y. Fujimoto, T. Kajino, and S. Kubono, *AIP Conf. Proc.* **1016** (2008).
- [2] S. Kubono, *Z. Phys.* **A349** (1994) 237.
- [3] S. Kubono, et al., *Nucl. Phys.* **A834** (2010) 647c.
- [4] Artemov et al., *Sov. J. Nucl. Phys.* 52 (1990) 408  
S. Kubono, *Nucl. Phys.* **A693** (2001) 221.
- [5] S. Kubono, Y. Yanagisawa, T. Teranishi, S. Kato, Y. Kishida, S. Michimasa, Y. Ohshiro, S. Shimoura, K. Ue, S. Watanabe, and N. Yamazaki, *Eur. Phys. J.* **A13** (2002) 217.
- [6] Y. Yanagisawa, S. Kubono, T. Teranishi, I. K. Ue, S. Michimasa, M. Notani, J.J. He, Y. Ohshiro, S. Shimoura, S. Watanabe, N. Yamazaki, H. Iwasaki, S. Kato, T. Kishida, T. Morikawa, and Y. Mizoi, *Nucl. Instr. Meth.* **A539** (2005) 74.
- [7] H. Yamaguchi, Y. Wakabayashi, G. Amadio, S. Hayakawa, H. Fujikawa, S. Kubono, J. J. He, A. Kim, and D. N. Binh, *Nucl. Instr. Meth.* **A 589** (2008) 150 .
- [8] H. Yamaguchi, T. Hashimoto, S. Hayakawa, D. N. Binh, D. Kahl, and S. Kubono, Y. Wakabayashi, T. Kawabata, and T. Teranishi, *Phys. Rev.* **C 83** (2011) 034306.
- [9] T. Yoshida, T. Kajino, H. Yokomakura, K. Kimura, A. Takamura, and D. H. Hartman, *Phys. Rev. Lett.* **96** (2006) 091101.
- [10] T. Suhara and Y. Kanada-En'yo, *Prog. Theor. Phys.* **123** (2010) 303.
- [11] M. Notani, et al., *Nucl. Phys.* **A746** (2004) 113.
- [12] A. Kim, N. H. Lee, I. S. Hahn, J. S. Yoo and M. H. Han, S. Kubono, H. Yamaguchi, S. Hayakawa, Y. Wakabayashi, D. N. Binh, H. Hashimoto, T. Kawabata, D. Kahl, Y. Kurihara, Y. K. Kwon, T. Teranishi, S. Kato, T. Komatsubara, B. Guo, G. Bing, W. P. Liu and Y. Wang, *J. Korean Phys. Soc.*, **57** (2010) 40.
- [13] C. Frohlich, et al., *Phys. Rev. Lett.* **96** (2006) 142502.
- [14] J. Pruet, R. D. Hoffman, S. E. Woosley, R. Buras, and H.-Th. Janka, *Astrophys. J.* **644** (2006) 1028.
- [15] S. Wanajo, *Astrophys. J.* **647** (2006) 1323.
- [16] S. Wanajo, H.-T. Janka, and S. Kubono, *Astrophys. J.* **729** (2011) 46.
- [17] G. Magkotsios, F.X. Timmes, A.L. Hungerford, C. L. Fryer, P.A. Young, M. Wiescher, *Astrophys. J. Suppl.* **191** (2010) 66.
- [18] R. Diehl, et al., Proc. *Origin of Matter and Evolution of Galaxies 2010*, eds. I. Tanihata, T. Shima, H.J. Ong, A. Tamii, T. Kishimoto, H. Toki, T. Kajino, and S. Kubono, *AIP Conf. Proc.* **1269** (2010) 144.
- [19] Dam G. Binh, to be published.
- [20] W. Gruhle and B. Kober, *Nucl. Phys.* **A286** (1977) 523.
- [21] A. Arima and S. Kubono, *Treatise on Heavy-Ion Science*, vol. **I**, Chapter 6, ed. by D. A. Bromley, Plenum Press (New York, 1984).
- [22] D.H. Feng, T. Udagawa, T. Tamura, *Nucl. Phys.* **A274** (1976) 262.
- [23] T. Takemasa H. Yoshida, *Nucl. Phys.* **A 304** (1978) 229.
- [24] S. Kubono, PhD thesis, University of Tokyo, 1975. H. Ohnuma, et al, *J. Phys. Soc. Japan*, 48 (1980) 1812.
- [25] M. Igarashi, TWO-FNR code, private communication.
- [26] S. Kubono, et al., *Phys. Rev. Lett.* **90** (2003) 062501.
- [27] E. D. Johnson, et al., *Phys. Rev. Lett.* **97** (2006) 192701.
- [28] F. Hammache, et al., Proc. *Symp. Physics of Unstable Nuclei*, World Scientific, (2008) 297.
- [29] R. Stokstadt, Proc. *Reactions between Complex Nuclei*, Nucl. Phys. conf. (1974) 352.
- [30] *Treatise on Heavy-Ion Science*, vol. 2, ed. by D. A. Bromley, Plenum Press (New York, 1984).
- [31] K. Morita, S. Kubono, et al., *Phys. Rev. Lett.* **55** (1985) 185.
- [32] C. Spitaleri, private communication.